Environmental Science and Ecotechnology 22 (2024) 100456

Contents lists available at ScienceDirect

Environmental Science and Ecotechnology

journal homepage: www.journals.elsevier.com/environmental-science-and-ecotechnology/

Original Research

Low-condensation diesel use contributes to winter haze in cold regions of China

Weiwei Song [a, *], Mengying Wang [a], Yixuan Zhao [a], Yu Bo [b, c], Wanying Yao [a], Ruihan Chen [a], Xianshi Wang [a], Xiaoyan Wang [d], Chunhui Li [d], Kebin He [b, e, f, **]

[a] *State Key Laboratory of Urban Water Resource and Environment, School of Environment, Harbin Institute of Technology, Harbin, 150090, China*
[b] *State Key Joint Laboratory of Environment Simulation and Pollution Control, School of Environment, Tsinghua University, Beijing, 100084, China*
[c] *Institute of Atmospheric Physics, Chinese Academy of Sciences, Beijing, 100029, China*
[d] *Harbin Ecological and Environmental Monitoring Center, Harbin, 150076, China*
[e] *Collaborative Innovation Center for Regional Environmental Quality, Beijing, 100084, China*
[f] *State Environmental Protection Key Laboratory of Sources and Control of Air Pollution Complex, Beijing, 100084, China*

ARTICLE INFO

Article history:
Received 25 September 2023
Received in revised form
15 July 2024
Accepted 16 July 2024

Keywords:
Low condensation diesel
Carbonaceous matter
Heavy metal
Dynamometer
Cold regions

ABSTRACT

The application of low-condensation diesel in cold regions with extremely low ambient temperatures (−14 to −29 °C) has enabled the operation of diesel vehicles. Still, it may contribute to heavy haze pollution in cold regions during winter. Here we examine pollutant emissions from low-condensation diesel in China. We measure the emissions of elemental carbon (EC), organic carbon (OC), and elements, including heavy metals such as arsenic (As). Our results show that low-condensation diesel increased EC and OC emissions by 2.5 and 2.6 times compared to normal diesel fuel, respectively. Indicators of vehicular sources, including EC, As, lead (Pb), cadmium (Cd), chromium (Cr), nickel (Ni), and manganese (Mn), increased by approximately 20.2−162.5% when using low-condensation diesel. Seasonal variation of vehicular source indicators, observed at road site ambient environments revealed the enhancement of $PM_{2.5}$ pollution by the application of low-condensation diesel in winter. These findings suggest that −35# diesel, a low-cetane index diesel, may enhance air pollution in winter, according to a dynamometer test conducted in laboratory. It raises questions about whether higher emissions are released if −35# diesel is applied to running vehicles in real-world cold ambient environments.

1. Introduction

Vehicle exhaust emission is a significant source of inhalable particulate matter (PM), particularly in urban areas [1,2]. These emissions release hazardous substances into the air, including PM-bound carbonaceous materials, heavy metals, volatile organic compounds (VOCs), and polycyclic aromatic hydrocarbons (PAHs). These pollutants degrade urban air quality and directly threaten residents' health. Vehicle exhaust emissions were responsible for approximately 12.5% of deaths in China attributed to long-term exposure to $PM_{2.5}$ in 2018 [3]. Epidemiological studies have revealed that prolonged exposure to PM from the exhaust has adverse health consequences, including cardiovascular disease-related fatalities, respiratory diseases, and childhood asthma [3,4]. The presence of potentially toxic elements (PTEs) in the environment, such as arsenic (As), cobalt (Co), chromium (Cr), cadmium (Cd), copper (Cu), nickel (Ni), lead (Pb), antimony (Sb), and zinc (Zn), has raised considerable concerns due to their high toxicity, persistence in the environment, and propensity to bioaccumulate [5,6]. In China, five heavy metals, specifically Cd, mercury (Hg), Cr, As, and Pb, were classified as hazardous air pollutants (HAPs) in 2019, emphasizing the need for risk management measures based on the updated HAPs list [7]. Elemental carbon (EC) and organic carbon (OC) contribute to the toxicity of PM, with potential health impacts such as disruptions in heart rate, lipid peroxidation of human bronchial epithelial cells, and elevated levels of plasma oxidative stress markers [8].

---

* Corresponding author.
** Corresponding author. State Key Joint Laboratory of Environment Simulation and Pollution Control, School of Environment, Tsinghua University, Beijing, 100084, China.
E-mail addresses: wwwsong@hit.edu.cn (W. Song), hekb@tsinghua.edu.cn (K. He).

https://doi.org/10.1016/j.ese.2024.100456

Temperature enhanced the emissions of toxic substances by resulting the low combustion efficiency, low catalyst performance, and possible operation under fuel-rich conditions [9,10]. Growing evidence has indicated a substantial increase in diesel vehicle emissions at low temperatures, heightening health risks [11,12]. These conditions notably boost the release of OC, EC, and PAHs from diesel trucks. Specifically, at low ambient temperatures (−20 to −13 °C), the emission factors (EFs) for EC from China II light-duty diesel trucks (LDDTs) and China IV LDDTs surpass those at 18–25 °C by 1.41 and 1.96 times, while the EFs for EC from China II heavy-duty diesel trucks (HDDTs) and China IV HDDTs exceed those at 18–25 °C by 1.93 and 1.73 times. Emissions of nitrogen oxides from gasoline vehicles are 67% greater in winter than in spring [13]. Vulnerable populations, including children, the elderly, and individuals with chronic illnesses are disproportionately affected by winter pollutants due to their weakened immunity and reduced resilience [14].

Low-condensation diesel oil is used in cold regions in the winter. Various studies represent the impact of diesel properties on hazardous emissions in ordinary temperatures. Viscosity, density, and cetane index were found to significantly impact emissions. The higher the kinematic viscosity of the fuel, the worse its fluidity. It is detrimental to the transport, atomization, and combustion of the fuel [15,16], which would increase hydrocarbon (HC) and PM emissions. Lower-density fuels may cause incomplete combustion and produce unburned HC, while a higher-density fuel with more heavy constituents would raise the emissions of CO_2 and PM [17]. Diesel with a high cetane index burns evenly, making it easy to start and produce a large output power, while diesel with a low cetane index ignites slowly, works unstably, and is prone to detonation [18,19]. It is necessary to select suitable fuels according to seasons and regions, and fuel properties. Hence, the selection of fuel is the first factor affecting the EFs of PM [20].

Thus far, there's few evidence to evaluate whether low-condensation diesel would enhance air pollution in winter. In this study, a dynamometer was applied to evaluate the characteristics of fine particle emissions from −35# low-condensation diesel. The investigation was conducted in a laboratory to avoid the influences of other factors, such as traffic conditions, road materials, driving custom, and emissions from other parts of vehicles. In vast regions with cold winters, −35# diesel is the fuel of choice. It has distinguishable properties (cetane index, density, viscosity, cold-filtered plugging point, flashing point, etc.) compared to 0# diesel used in ordinary temperatures. Carbonaceous matters (elemental carbon, organic carbon, and total carbon, TC) and heavy metals (vanadium, V, Cr, manganese, Mn, Ni, Cu, Zn, Cd, Pb, and molybdenum, Mo) are tested. The research aims to determine whether low-condensation diesel is a significant driver of increased air pollution in cold winter.

2. Methods and materials

2.1. Experimental design

To investigate the properties of $PM_{2.5}$-bonded chemicals from low condensation diesel fuel, a dynamometer was used to test the operational cycles of the diesel engine. The test was conducted in the laboratory to avoid confounders such as interruptions to traffic systems, driving custom, road materials, etc. Hence, the conditions of emission tests could be more controllable, accurate, and repeatable. The exhaust dilution sampling system was equipped with an exhaust pipe to collect the $PM_{2.5}$ samples (Fig. 1).

The emissions from two types of diesel fuel were examined. The target of determination was low-condensation diesel (−35# diesel). 0# diesel, which is used at ordinary ambient temperature, is applied to compare with −35# diesel. The $PM_{2.5}$-bonded chemicals included carbonaceous matter (TC, OC, and EC), heavy metals (V, Cr, Mn, Ni, Cu, Zn, Cd, Pb, and Mo), and the non-metallic element As.

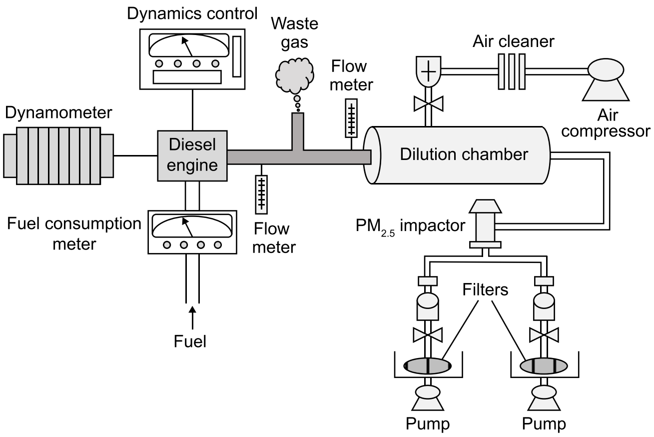

Fig. 1. The exhaust sampling dilution system. The system consists of a dilution chamber, a digital control module, a $PM_{2.5}$ impactor, an air compressor, an air cleaner, flow meters, pumps, and heaters. The exhaust is diluted before going through the $PM_{2.5}$ impactor. Before entering the dilution chamber, the compressed air is cleaned. To prevent the loss of particles due to condensation, the diluted air is heated before passing through the $PM_{2.5}$ impactor.

This study compared the differences in emissions from the combustion of −35# and 0# diesel under the same experimental conditions. Hence, the tests were conducted at 23–25 °C in the dynamometer laboratory. Notably, the emissions from −35# diesel would be even worse in ambient environments below −20 °C. The low temperature would lead to lower combustion efficiency in the engine, resulting in higher actual emissions than those measured in the laboratory.

2.2. Fuel properties

In China, diesel fuel is classified according to China GB19147-2016 [21]. Specifically, −35# diesel is a typical low-condensation diesel used in the temperature range of −14 to 29 °C. Conversely, 0# diesel is used in temperatures above 4 °C. Compared to 0# diesel, −35# diesel has a lower cetane index, density, viscosity, and flash point (Table 1).

2.3. Test engine and working modes

The tested engine JX493ZLQ has a power output of 75 kW, uses high-pressure common rail electronic injection technology, equipped with a supercharged intercooler. According to the working conditions, the electronic control unit (ECU) controls the fuel pressure in the high-pressure oil rail through a high-pressure oil pump and controls the pressure relief valve on the nozzle to select the best fuel injection phase and rule. It is a four-cylinder diesel engine with a displacement of 2.771 L (Supplementary Material

Table 1
Properties of −35# and 0# diesel.

Fuel properties	−35#	0#
Application temperature (°C)	−14 to −29	>4
Density (kg m^{-3})	790–840	810–850
Cetane index	≥45	≥49
20 °C viscosity (mm^2 s^{-1})	1.8–7.0	3.0–8.0
Sulfur content (mg L^{-1})	10	10
Cold filtered plugging point (°C)	−29	4
Flash point (°C)	≥45	≥60

Table S1). The engines of the series are mostly applied to light-duty trucks.

The test cycle is based on the specifications of the tested engine and follows the calculation method of the European Stability Cycle (ESC) (Supplementary Material Fig. S1). The ESC defines high speed as 70% of the declared maximum net power, while low speed is 50% of the maximum net power. The detailed calculations of speeds are shown in the Supplementary Materials (Supplementary Material equations S1–S3). The test cycle featured three speeds (A, B, and C represent engine speeds of 1500, 2000, and 2500 r min^{-1}, respectively) and three loads (25%, 50%, and 75%), resulting in nine operating points. Three samples were collected for each operating point, and the same driving mode was used in testing both fuels.

2.4. Sampling and analysis

The exhaust particles from diesel engine emissions were collected by an exhaust sampling dilution system (Fig. 1). Duplicate samples were collected at the same operational cycles on a quartz filter and a Teflon filter for 10 min (23–25 °C, relative humidity 50%). The quartz filter was prepared and cut into a circular sampling film with a diameter of 47 mm. It was then placed in a muffle furnace and calcined at 450 °C for 24 h. After completely cooling the filter, it was enclosed in prepared foil with one open end. The wrapped filters were placed in a desiccator for 48 h.

The carbonaceous matter was determined by the DRI Model 2001A OC/EC analyzer (Desert Research Institute, USA) employing the Improve Temperature Program (reflectance method). A 633 nm laser irradiated the sample and measured the change in reflectance, enabling the distinction between OC and EC. The carbon contents were quantified using a flame ionization detector (FID).

Spectroscopic method (ICP-MS) were employed to identify and determine the amounts of chemical elements (V, Cr, Mn, Ni, Cu, Zn, As, Mo, Cd, and Pb) in the $PM_{2.5}$ samples. The samples were digested in a polytetrafluoroethylene digestion tank with 6 mL nitric acid, 2 mL hydrogen peroxide, and 100 μL hydrofluoric acid [22,23]. The polytetrafluoroethylene digestion tank was sealed and placed in a high-pressure autoclave, where it was digested for 8 h under high temperature and high pressure. Subsequently, deionized water (15 mL) was added to each sample, and the measurements were performed using an Agilent 7700 ICP-MS spectrometer.

2.5. Computing methods

2.5.1. Emission factors

EFs were calculated according to the mass of chemicals in samples and the corresponding diesel consumption (equation (1)):

$$EF_{ij} = \frac{M_j \times 2 \times \phi}{V \times \rho_i} \tag{1}$$

Where i represents the type of diesel, j represents the determined chemical compound, M is the mass of chemicals j in the samples (mg or μg), ϕ is the sampling ratio (the sampling volume divided by the total emission volume from the exhaust), V is the volume of diesel i (L), ρ is the density of diesel i (kg L^{-1}), and EF_{ij} is the EF of chemical j from the emissions of diesel i (μg kg^{-1}).

2.5.2. Principal component analysis

Principal component analysis (PCA) is a multivariate statistical method applied to determine correlation in variable indexes in agriculture, biology, and other research fields. In PCA, new variables (principal components [PCs]) are derived according to the original variables. PCs are linear combinations of the original variables and retain the original variables to be as informative as possible, and they are orthogonal. The percentage of variance that the PCs can explain reflects the percentage of data that can be interpreted, and most of the information within the initial variable is compressed into the first component (PC1) [24]. The datasets of measured chemical elements in $PM_{2.5}$ samples were subjected to factor analysis with varimax rotation using Statistical Package for the Social Sciences (SPSS) version 25. Graphs of the analyzed data were plotted and modified on http://www.cloud.biomicroclass.com/.

2.6. Chemical composition of $PM_{2.5}$ in ambient environments

To analyze the emissions of chemicals from −35# diesel, the ambient concentrations of corresponding chemicals emitted in January 2024 (winter) and August 2023 (summer) were adapted from the Atmospheric Super Site in Harbin, Heilongjiang Province, China (45.78° N, 126.53° E). Metal element (Mn, As, Ni, Cr, Pb, and Cd) were analyzed by a real-time ambient multi-metals monitoring system (Xact-625, Cooper Environmental, USA). The semi-continuous OC-EC field analyzer measured EC and OC mass concentrations (Mode 14, Sunset Laboratory, Portland, OR, USA). The real-time source apportionment results for $PM_{2.5}$ were analyzed using the online Single Particle Aerosol Mass Spectrometry (SPAMS 0515) program.

3. Results and discussion

3.1. Negative effects of low-condensation diesel on carbonaceous matter in fine particle emissions

The combustion of low-condensation diesel (−35#) led to the higher emission of carbonaceous matter in fine particles than the combustion of 0# diesel (above 4 °C). The comprehensive EFs (EF_{COMP}) of TC, EC, and OC were 9.78, 8.57, and 1.21 mg kg^{-1} under the 13-cycle operating condition. The EF_{COMP} of TC, OC, and EC from low-cetane diesel were 2.51, 2.62, and 2.50 times higher than that from combusting 0# diesel (Fig. 2). EC is composed of soot formed by incomplete combustion. Thus, the OC emissions correlated with the physicochemical properties of the fuel, specifically the unburned fuel or lubricant oil. OC is generated by unburned fuel, lubricating oil, and condensation during the cooling process through the exhaust pipe [12,25,26]. The cetane index of −35# diesel is lower than that of 0# diesel, which reduces the evenness and efficiency of fuel combustion in engines. It revealed the initiation of higher carbonaceous emissions from combusting −35# diesel. The cetane index is a significant factor in carbonaceous emissions. These results show that air pollutants produced by incomplete combustion decrease with an increase in the cetane index of diesel fuel [27]. Moreover, the EC/OC ratios of −35# and 0# diesel were 6.84 and 7.56, respectively (Fig. 2). The OC proportion of −35# diesel emissions was higher than that of 0# diesel. It indicates that also emissions of both EC and OC were increased by using −35# diesel, and the proportion of OC in TC from −35# diesel was higher than that from 0#.

Engine operating conditions, fuel composition, and type have a significant influence on the formation of EC and OC [1,26,28–30]. Use of −35# diesel resulted in significantly higher emissions of EC and OC at various engine working cycles (excluding the working cycle with the highest speed and load, C75%). The 25% and 50% loads, the EC/OC ratios of −35# diesel emissions were lower, but when the load was up to 75%, the results were inverse. When engine speeds increased, the EC emissions decreased for both −35# and 0# diesel, and the differences in EC emissions between the two types of diesels decreased. This aligns with the relationship between engine speed and combustion efficiency, indicating that higher speeds enhance air swirl motion in the combustion

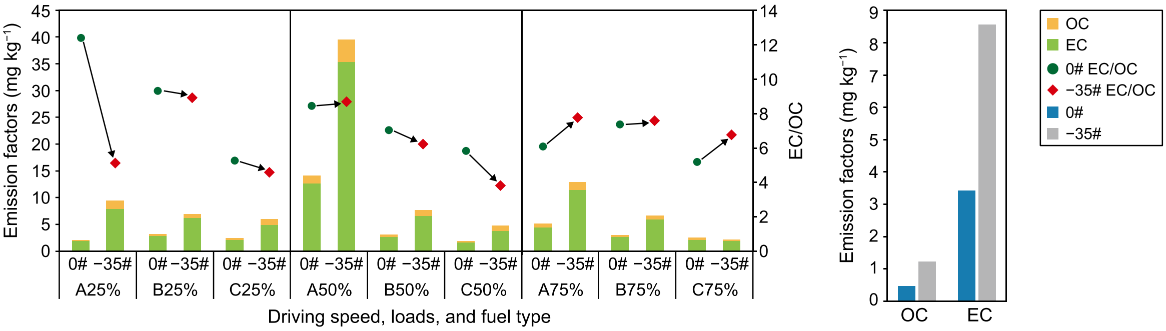

Fig. 2. Emission factors (EFs) of carbonaceous matters from −35# and 0# diesel by engine working cycles and comprehensive EFs of 13-driving cycles (blue and grey columns). A, B, and C represent engine speeds of 1500, 2000, and 2500 r min^{-1}; three speeds (A, B, and C) and three loads (25%, 50%, and 75%) result in nine operating points.

chamber, promoting fuel evaporation, atomization, air mixing, and combustion. Lower engine speeds can weaken air swirls, leading to reduced thermal efficiency.

Furthermore, emissions of both EC and OC at A50% were much higher than in other working cycles. When engine speed was the same, the loads of A50% were higher, and the combustion was not as sufficient as at A25%, which resulted in higher emissions than at A25%. Compared to A75%, when the loads were up to 75%, with high gas intake and engine operation temperature, the combustion was relatively sufficient; hence, the emissions at A75% would be lower than A50%. Thus at the A50%, it relatively easier to produce high pollution.

3.2. *Influences of low-condensation diesel on heavy metals in fine particle emissions*

Fuel combustion is the key driver in the abundance of heavy metals in diesel exhaust [31,32]. The dominant elements in heavy metal emissions from −35# and 0# diesel is of similarity. Emissions of Mo were the highest compared to other elements. Aside from Mo, Zn, Ni, and Cr were dominant elements from diesel exhaust else (Supplementary Materials Table S2). Above all, EF$_{COMP}$ showed that heavy metals from −35# diesel combustion were higher than those from 0# diesel, except for Zn (Supplementary Materials Fig. S2). For the individual components, the EF of Cd increased the most (89.93%), followed by Pb (52.55%), Cr (46.86%), Ni (36.89%), V (33.62%), As (32.98%), Mn (20.22%), and Cu (17.84%) (Fig. 3). In the perspective of health risks, all these heavy metals have strong biotoxicity and are associated with carcinogenic risk. Cd and As have mutagenic potential, while Pb results in fetal toxicity. The increase in emissions from the combustion of −35# diesel would enhance the risk of human exposure to heavy metals in the winter.

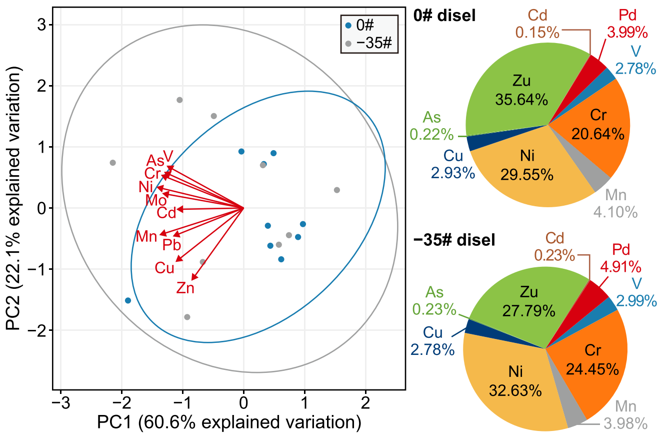

Fig. 3. PCA analysis according to fuel type (−35# and 0#). The heavy metals' total emission factors of 0# diesel and −35# diesel were 94.33 and 116.94 μg kg^{-1}. The pie charts represent the proportions of elements in total heavy metals.

The cumulative contribution rate of PC1 and the second component (PC2) in PCA could explain over 80% of the variance, ensuring enough information on the principal components [33]. Scatter plots of samples revealed the similarities in the elements from 0# and −35# diesel combustion (Fig. 3). The distance between samples in a group indicates the similarities in emission properties. The characteristics of the elements in the 0# diesel group were closer than those in the −35# diesel group.

The emissions of V, Cr, Mn, Ni, and As statistically correlated with the engine working cycles (Supplementary Materials Table S3). At the 25% and 50% loads, the emissions of V, Cr, Mn, Ni, and As from −35# diesel were higher than those from 0# diesel. The results were inverse at the 75% load (Fig. 4).

Diesel fuels emit a large amount of Mo due to the higher content of Mo in diesel fuels [34]. Compared to other detected metals, the Mo content from both 0# and −35# diesel was much higher, consistent with previous studies' results [35]. The amount of Mo from −35# diesel exhaust was higher (116.46 μg kg^{-1}) than that from 0# diesel (92.27 μg kg^{-1}). Mo is normally added to diesel as a lubricant, antioxidant, and preservative. From the perspective of human health, the excessive intake of Mo causes metabolic disorders, myocardial hypoxia, hyperosteogeny, etc. Hence, increased Mo emissions is a significant health risk.

3.3. *Enhanced pollution resulting from vehicular diesel emissions in the winter*

In Northeast China, heavy pollution episodes appear mostly in winter, owing to the increased emissions of pollutants resulting from increased fuel combustion (e.g., coal combustion, biomass burning, or vehicular emissions) in response to colder weather [23,36,37]. We took Harbin as an example, as it is a typical city in the cold region of Northeast China. Heavy pollution occurs exclusively in the winter, and PM$_{2.5}$ is the dominant pollutant that induces haze pollution episodes [36]. Higher concentrations of PM$_{2.5}$ in winter, while lower in summer appeared periodically (Fig. 5a). Increased evidences indicate that vehicle emissions become a significant source of PM$_{2.5}$ pollution [23,37]. The latest source apportionment results from a heavy pollution day showed that the contribution of vehicular sources is up to 20% of the PM$_{2.5}$ pollution (Fig. 5b). Owing to the Cleaning Heat Programs launched in Northeast China, emissions from coal combustion have been reduced gradually, by inference, emissions of vehicles in winters would become a serious concernment to heavy pollution and the

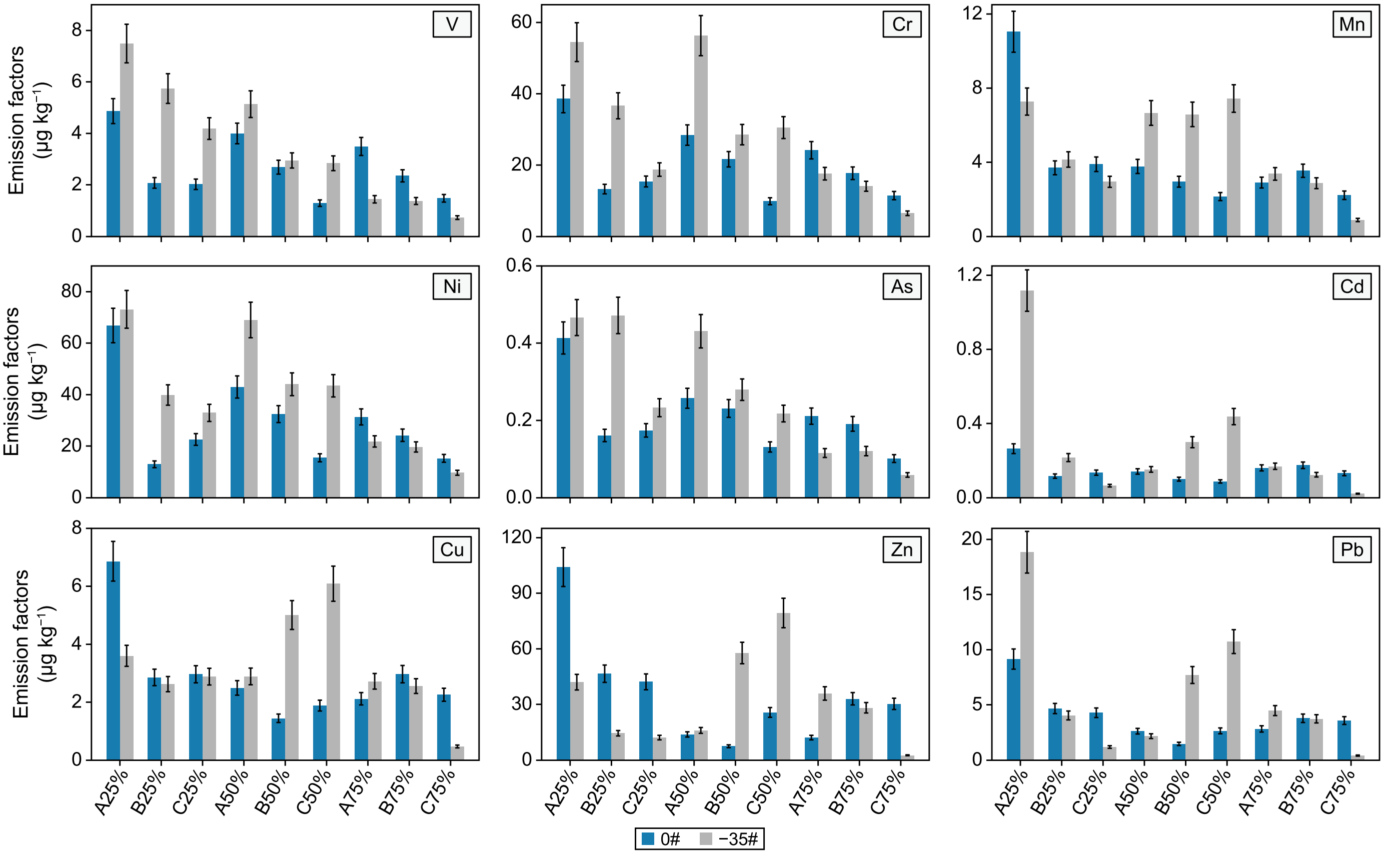

Fig. 4. Emissions of heavy metals from −35# and 0# diesel by engine working cycles. A, B, and C represent engine speeds of 1500, 2000, and 2500 r min^{-1}; three speeds (A, B, and C) and three loads (25%, 50%, and 75%) result in nine operating points.

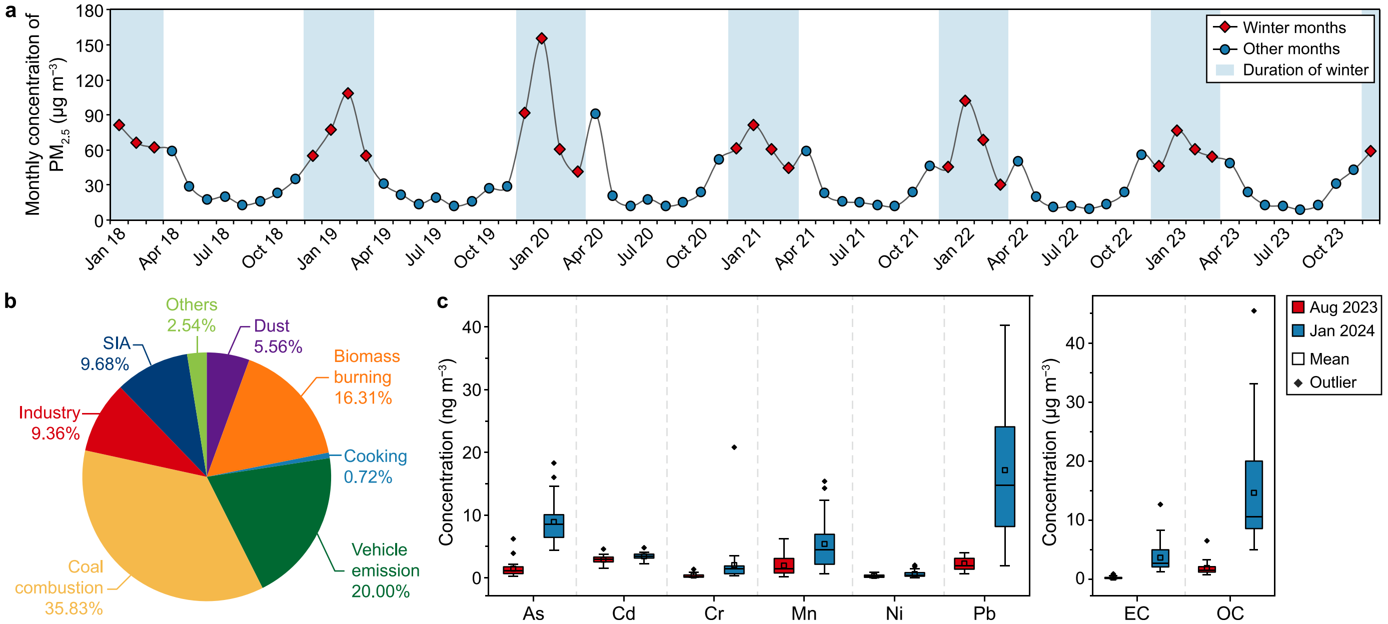

Fig. 5. Impacts of diesel emissions on the environment in winter. **a**, Monthly concentrations of PM$_{2.5}$ in 2018–2023. **b**, Source apportionment of PM$_{2.5}$ on a winter day (January 2, 2024) of a heavy haze pollution episode (Air Quality Index [AQI] = 205). Data are collected from Harbin's Atmospheric Supersite. **c**, The comparison of chemical compounds in PM$_{2.5}$ related to vehicular emissions in summer and winter.

chemical reactions in the air.

On-road vehicular emissions tests have confirmed that pollutant emissions are higher in the winter than summer (Supplementary Materials Fig. S3) [12]. These increased emissions could be induced by the applied fuel in winter, the effects of cold weather on the operation of engines, the coverage of snow on the road, etc. Low-condensation diesel is used in the winter (−35# diesel), a key factor associated with emissions. To avoid the influences of other factors, tests of −35# diesel fuel combustion in the lower temperatures were carried out in a laboratory with a diesel engine dynamometer. As a result, the indicators of vehicular sources, including EC, OC, As, Pb, Cd, Cr, Ni, and Mn increased by approximately 20.22−162.48% (Supplementary Materials Table S4). The corresponding concentrations of those elements all went up in winter (Fig. 5c). The growth of Pb, As, Mn, and carbonaceous matters are notably severe. It revealed the negative impacts of using the low condensation diesel. Associated with the results of on−road emission tests, the emissions would be even worse if the −35# diesel is used in a cold working environment.

Furthermore, Pb and Mn (1316 and 4249.5 μg, respectively) were detected in emissions from a liter of diesel. They were the dominant elements in the diesel's chemical profile [34]. The chemical compositions of $PM_{2.5}$ in the ambient environment were determined in both cold winter and summer at a roadside sampling site in Northeast China [22]. Ambient Pb and Mn in $PM_{2.5}$ were mostly emitted from vehicular sources. Concentrations of Pb and ambient $PM_{2.5}$ were seven and two times higher in the winter than in the summer, respectively (Fig. 5c, Supplementary Materials Table S5). On these occasions, Pb and Mn were identified as indicators of increased pollution from the combustion of −35# diesel.

4. Conclusions

The application of −35# diesel fuel has been found to increase the emissions of carbonaceous matter and heavy metals, such as Mo, As, Pb, Cd, Cr, and Mn. In fact, proportions of these compounds emitted from the combustion of −35# diesel fuel are much higher than emissions from 0# diesel fuel. Supporting the real-time monitoring data gathered at the Atmospheric Super Site, it revealed that the enhanced emissions from low-condensation diesel would contribute significantly to heavy pollution episodes. These findings raise questions regarding the impact of the lower cetane index of −35# diesel on increased emissions. Further quantitative analysis is necessary to fully understand the influence of the cetane index on emissions.

Certain implications of the study should be considered: (1) The empirical data reported the direct emissions from a diesel engine and aimed to represent the effects of −35# used in the winter. If equipped with aftertreatment devices, emissions would be reduced effectively. Thus far, the reduction efficiency of aftertreatment devices on −35# diesel has not been quantitatively evaluated. The effects of a low-temperature ambient environment on the working efficiency of aftertreatment devices should also be considered; (2) Engines that comply with China VI standards differ from their predecessors. The present study focused on the characteristics of −35# diesel in engines designed prior to the institution of China VI standards. Further investigations are needed to examine the emissions from China VI engines and provide quantified scientific evidence to support the elimination of vehicles with high emissions; (3) Due to the higher vehicular emissions in winter, alternative energy fuels are required. According to the technologies currently in use, appropriate aftertreatment and alternative energy vehicles are urgently needed to improve the air quality of cold regions.

CRediT authorship contribution statement

Weiwei Song: Writing - Review & Editing, Writing - Original Draft, Methodology, Funding Acquisition, Conceptualization. **Mengying Wang:** Formal Analysis, Data Curation, Methodology, Writing - Review & Editing. **Yixuan Zhao:** Methodology, Data curation. **Yu Bo:** Investigation, Formal Analysis. **Wanying Yao:** Data Curation. **Ruihan Chen:** Methodology. **Xianshi Wang:** Investigation. **Xiaoyan Wang:** Resources, Investigation. **Chunhui Li:** Resources, Methodology. **Kebin He:** Supervision, Conceptualization.

Declaration of competing interest

The authors declare that they have no known competing financial interests or personal relationships that could have appeared to influence the work reported in this paper.

Acknowledgements

This work Is supported by the National Natural Science Foundation of China (51778181) and an Open Project of the State Key Laboratory of Urban Water Resource and Environment, Harbin Institute of Technology (No. ES201908).

Appendix A. Supplementary data

Supplementary data to this article can be found online at https://doi.org/10.1016/j.ese.2024.100456.

References

[1] M. Wang, P. Tian, L. Wang, Z. Yu, T. Du, Q. Chen, X. Guan, Y. Guo, M. Zhang, C. Tang, Y. Chang, J. Shi, J. Liang, X. Cao, L. Zhang, High contribution of vehicle emissions to fine particulate pollution in Lanzhou, Northwest China based on high-resolution online data source appointment, Sci. Total Environ. 798 (2021) 149310, https://doi.org/10.1016/j.scitotenv.2021.149310.

[2] A. Tripathi, A.K. Agarwal, Characterisation of particulates and trace metals emitted by a dimethyl ether-fuelled genset engine prototype, Environ. Pollut. 329 (2023) 121649, https://doi.org/10.1016/j.envpol.2023.121649.

[3] Z. Luo, Y. Wang, Z. Lv, T. He, J. Zhao, Y. Wang, F. Gao, Z. Zhang, H. Liu, Impacts of vehicle emission on air quality and human health in China, Sci. Total Environ. 813 (2022) 152655, https://doi.org/10.1016/j.scitotenv.2021.152655.

[4] G. Touloumi, K. Katsouyanni, D. Zmirou, J. Schwartz, C. Spix, A.P. de Leon, A. Tobias, P. Quennel, D. Rabczenko, L. Bacharova, L. Bisanti, J.M. Vonk, A. Ponka, Short-term effects of ambient oxidant exposure on mortality: a combined analysis within the APHEA project. Air Pollution and Health: a European Approach, Am. J. Epidemiol. 146 (1997) 177−185, https://doi.org/10.1093/oxfordjournals.aje.a009249.

[5] E.N. Kelly, D.W. Schindler, V.L. St Louis, D.B. Donald, K.E. Vladicka, Forest fire increases mercury accumulation by fishes via food web restructuring and increased mercury inputs, Proc. Natl. Acad. Sci. USA 103 (2006) 19380−19385, https://doi.org/10.1073/pnas.0609798104.

[6] I. Campos, C. Vale, N. Abrantes, J.J. Keizer, P. Pereira, Effects of wildfire on mercury mobilisation in eucalypt and pine forests, Catena 131 (2015) 149−159, https://doi.org/10.1016/j.catena.2015.02.024.

[7] MEE and NHC, List of Hazardous Air Pollutants, EPA (n.d.).

[8] World Health Organization. Regional Office for Europe, Air Quality Guidelines: Global Update 2005: Particulate Matter, Ozone, Nitrogen Dioxide and Sulfur Dioxide, World Health Organization, Regional Office for Europe, 2006. https://apps.who.int/iris/handle/10665/107823. (Accessed 4 September 2023).

[9] B. Zielinska, J. Sagebiel, J.D. McDonald, K. Whitney, D.R. Lawson, Emission rates and comparative chemical composition from selected in-use diesel and gasoline-fueled vehicles, J. Air Waste Manag. Assoc. 54 (2004) 1138−1150, https://doi.org/10.1080/10473289.2004.10470973.

[10] E. Nam, S. Kishan, R.W. Baldauf, C.R. Fulper, M. Sabisch, J. Warila, Temperature effects on particulate matter emissions from light-duty, gasoline-powered motor vehicles, Environ. Sci. Technol. 44 (2010) 4672−4677, https://doi.org/10.1021/es100219q.

[11] S.K. Grange, N.J. Farren, A.R. Vaughan, R.A. Rose, D.C. Carslaw, Strong temperature dependence for light-duty diesel vehicle NOx emissions, Environ. Sci. Technol. 53 (2019) 6587−6596, https://doi.org/10.1021/acs.est.9b01024.

[12] W.W. Song, W.X. Fang, H. Liu, W.L. Li, Z. Zhang, C.H. Li, D. Yu, Q. Zhao, X.S. Wang, K.B. He, Enhanced diesel emissions at low ambient temperature: hazardous materials in fine particles, J. Hazard Mater. 449 (2023) 131011, https://doi.org/10.1016/j.jhazmat.2023.131011.

[13] A.J. Cohen, M. Brauer, R. Burnett, H.R. Anderson, J. Frostad, K. Estep, K. Balakrishnan, B. Brunekreef, L. Dandona, R. Dandona, V. Feigin, G. Freedman, B. Hubbell, A. Jobling, H. Kan, L. Knibbs, Y. Liu, R. Martin, L. Morawska, C.A. Pope, H. Shin, K. Straif, G. Shaddick, M. Thomas, R. Van Dingenen, A. Van Donkelaar, T. Vos, C.J.L. Murray, M.H. Forouzanfar, Estimates and 25-year trends of the global burden of disease attributable to ambient air pollution: an analysis of data from the Global Burden of Diseases Study 2015, Lancet 389 (2017) 1907−1918, https://doi.org/10.1016/S0140-6736(17)

30505-6.

[14] World Health Organization, Ambient Air Pollution: a Global Assessment of Exposure and Burden of Disease, World Health Organization, 2016. https://apps.who.int/iris/handle/10665/250141. (Accessed 4 September 2023).

[15] D. Tutunea, Study of the variation of kinematic viscosity and density of various biodiesel blends with temperature, Rev. Chem. 69 (2018) 1645–1648.

[16] D. Mei, L. Zuo, Q. Zhang, M. Gu, Y. Yuan, J. Wang, Assessment on combustion and emissions of diesel engine fueled with partially hydrogenated biodiesel, J. Energy Eng. 146 (2020) 04019038, https://doi.org/10.1061/(ASCE)EY.1943-7897.0000637.

[17] H. Liu, J. Ma, F. Dong, Y. Yang, X. Liu, G. Ma, Z. Zheng, M. Yao, Experimental investigation of the effects of diesel fuel properties on combustion and emissions on a multi-cylinder heavy-duty diesel engine, Energy Convers. Manag. 171 (2018) 1787–1800, https://doi.org/10.1016/j.enconman.2018.06.089.

[18] A.S. Mohammed, S.M. Atnaw, A.V. Ramaya, G. Alemayehu, A comprehensive review on the effect of ethers, antioxidants, and cetane improver additives on biodiesel-diesel blend in CI engine performance and emission characteristics, J. Energy Inst. 108 (2023) 101227, https://doi.org/10.1016/j.joei.2023.101227.

[19] Fengwei Li, Effect of diesel engine performance on vehicle engine, Guangdong Chemical Industry 42 (19) (2015) 73–74.

[20] T. Jin, J. JinHU, Z. Li, Study on quantitative effects of four important factors on diesel engine particulate emission factors, Acta Sci. Circumstantiae 38 (12) (2018) 4630–4635, https://doi.org/10.13671/j.hjkxxb.2018.0333.

[21] General Administration of Quality Supervision, Inspection and Quarantine of the People's Republic of China, Standardization Administration: Automobile diesel fuels. GB19147-2016.https://std.samr.gov.cn/.

[22] M.O.A. Mohammed, W. Song, L. Liu, W. Ma, Y.-F. Li, F. Wang, M.A.E.M. Ibrahim, M. Qi, A.A. Elzaki, N. Lv, Distribution patterns and characterization of outdoor fine and coarse particles, Atmos. Pollut. Res. 7 (2016) 903–914, https://doi.org/10.1016/j.apr.2016.05.001.

[23] W. Fang, W. Song, L. Liu, G. Chen, L. Ma, Y. Liang, Y. Xu, X. Wang, Y. Ji, Y. Zhuang, A.H. Boubacar, Y. Li, Characteristics of indoor and outdoor fine particles in heating period at urban, suburban, and rural sites in Harbin, China, Environ. Sci. Pollut. Res. 27 (2020) 1825–1834, https://doi.org/10.1007/s11356-019-06640-7.

[24] L. Li, J. Zhao, C. Wang, C. Yan, Comprehensive evaluation of robotic global performance based on modified principal component analysis, Int. J. Adv. Rob. Syst. 17 (2020) 172988141989688, https://doi.org/10.1177/1729881419896881.

[25] J.-H. Tsai, S.-J. Chen, K.-L. Huang, Y.-C. Lin, W.-J. Lee, C.-C. Lin, W.-Y. Lin, PM, carbon, and PAH emissions from a diesel generator fuelled with soy-biodiesel blends, J. Hazard Mater. 179 (2010) 237–243, https://doi.org/10.1016/j.jhazmat.2010.02.085.

[26] T. Lu, C.S. Cheung, Z. Huang, Investigation on particulate oxidation from a DI diesel engine fueled with three fuels, Aerosol. Sci. Technol. 46 (2012) 1349–1358, https://doi.org/10.1080/02786826.2012.713534.

[27] W. Chen, F. Wu, J. Wang, Effect of cetane numberon combustion and emission of a euro-IV diesel engine, Chin. Intern. Combust. Engine Eng. 29 (06) (2008) 1–5.

[28] C.-B. Kweon, S. Okada, D.E. Foster, M.-S. Bae, J.J. Schauer, Effect of engine operating conditions on particle-phase organic compounds in engine exhaust of a heavy-duty direct-injection (D.I.) diesel engine, 2003-01–0342, https://doi.org/10.4271/2003-01-0342, 2003.

[29] S.S. Lim, T. Vos, A.D. Flaxman, G. Danaei, K. Shibuya, H. Adair-Rohani, M.A. AlMazroa, M. Amann, H.R. Anderson, K.G. Andrews, M. Aryee, C. Atkinson, L.J. Bacchus, A.N. Bahalim, K. Balakrishnan, J. Balmes, S. Barker-Collo, A. Baxter, M.L. Bell, J.D. Blore, F. Blyth, C. Bonner, G. Borges, R. Bourne, M. Boussinesq, M. Brauer, P. Brooks, N.G. Bruce, B. Brunekreef, C. Bryan-Hancock, C. Bucello, R. Buchbinder, F. Bull, R.T. Burnett, T.E. Byers, B. Calabria, J. Carapetis, E. Carnahan, Z. Chafe, F. Charlson, H. Chen, J.S. Chen, A.T.-A. Cheng, J.C. Child, A. Cohen, K.E. Colson, B.C. Cowie, S. Darby, S. Darling, A. Davis, L. Degenhardt, F. Dentener, D.C.D. Jarlais, K. Devries, M. Dherani, E.L. Ding, E.R. Dorsey, T. Driscoll, K. Edmond, S.E. Ali, R.E. Engell, P.J. Erwin, S. Fahimi, G. Falder, F. Farzadfar, A. Ferrari, M.M. Finucane, S. Flaxman, F.G.R. Fowkes, G. Freedman, M.K. Freeman, E. Gakidou, S. Ghosh, E. Giovannucci, G. Gmel, K. Graham, R. Grainger, B. Grant, D. Gunnell, H.R. Gutierrez, W. Hall, H.W. Hoek, A. Hogan, H.D. Hosgood, D. Hoy, H. Hu, B.J. Hubbell, S.J. Hutchings, S.E. Ibeanusi, G.L. Jacklyn, R. Jasrasaria, J.B. Jonas, H. Kan, J.A. Kanis, N. Kassebaum, N. Kawakami, Y.-H. Khang, S. Khatibzadeh, J.-P. Khoo, C. Kok, F. Laden, R. Lalloo, Q. Lan, T. Lathlean, J.L. Leasher, J. Leigh, Y. Li, J.K. Lin, S.E. Lipshultz, S. London, R. Lozano, Y. Lu, J. Mak, R. Malekzadeh, L. Mallinger, W. Marcenes, L. March, R. Marks, R. Martin, P. McGale, J. McGrath, S. Mehta, Z.A. Memish, G.A. Mensah, T.R. Merriman, R. Micha, C. Michaud, V. Mishra, K.M. Hanafiah, A.A. Mokdad, L. Morawska, D. Mozaffarian, T. Murphy, M. Naghavi, B. Neal, P.K. Nelson, J.M. Nolla, R. Norman, C. Olives, S.B. Omer, J. Orchard, R. Osborne, B. Ostro, A. Page, K.D. Pandey, C.D. Parry, E. Passmore, J. Patra, N. Pearce, P.M. Pelizzari, M. Petzold, M.R. Phillips, D. Pope, C.A. Pope, J. Powles, M. Rao, H. Razavi, E.A. Rehfuess, J.T. Rehm, B. Ritz, F.P. Rivara, T. Roberts, C. Robinson, J.A. Rodriguez-Portales, I. Romieu, R. Room, L.C. Rosenfeld, A. Roy, L. Rushton, J.A. Salomon, U. Sampson, L. Sanchez-Riera, E. Sanman, A. Sapkota, S. Seedat, P. Shi, K. Shield, R. Shivakoti, G.M. Singh, D.A. Sleet, E. Smith, K.R. Smith, N.J. Stapelberg, K. Steenland, H. Stöckl, L.J. Stovner, K. Straif, L. Straney, G.D. Thurston, J.H. Tran, R.V. Dingenen, A. van Donkelaar, J.L. Veerman, L. Vijayakumar, R. Weintraub, M.M. Weissman, R.A. White, H. Whiteford, S.T. Wiersma, J.D. Wilkinson, H.C. Williams, W. Williams, N. Wilson, A.D. Woolf, P. Yip, J.M. Zielinski, A.D. Lopez, C.J. Murray, M. Ezzati, A comparative risk assessment of burden of disease and injury attributable to 67 risk factors and risk factor clusters in 21 regions, 1990–2010: a systematic analysis for the Global Burden of Disease Study 2010, Lancet 380 (2012) 2224–2260, https://doi.org/10.1016/S0140-6736(12)61766-8.

[30] M.A. Ghadikolaei, C.S. Cheung, K.-F. Yung, Study of combustion, performance and emissions of a diesel engine fueled with ternary fuel in blended and fumigation modes, Fuel 235 (2019) 288–300, https://doi.org/10.1016/j.fuel.2018.07.089.

[31] T. Pulles, H. Denier Van Der Gon, W. Appelman, M. Verheul, Emission factors for heavy metals from diesel and petrol used in European vehicles, Atmos. Environ. 61 (2012) 641–651, https://doi.org/10.1016/j.atmosenv.2012.07.022.

[32] J.C. Ge, G. Wu, G. Xu, J.H. Song, N.J. Choi, Synthesis of polyvinyl alcohol/coal fly ash hybrid nano-fiber membranes for adsorption of heavy metals in diesel fuel, Nanomaterials 13 (2023) 1674, https://doi.org/10.3390/nano13101674.

[33] Y. Yuan, Y. Zhou, J. Sun, J. Deng, Y. Bai, J. Wang, Y. Lu, Determination and principal component analysis of mineral elements based on ICP-OES in Nitraria roborowskii fruits from different regions, China J. Chin. Mater. Med. 42 (2017) 2334–2338, https://doi.org/10.19540/j.cnki.cjcmm.20170412.002.

[34] X. QI, X. Zhu, Q. Gao, Laboratory Simulation Study on the Distribution of Heavy Metals and Polycyclic Aromatic Hydrocarbons in Marine Aerosol Affected by Crude Oil and Diesel Leakage, JournalofFudan University (NaturalScience) (n.d.). https://doi.org/DOI:10.15943/j.cnki.fdxb-jns.20230519.001.

[35] C.-Y. Kuo, H.-C. Chen, F.-C. Cheng, L.-R. Huang, P.-S. Chien, J.-Y. Wang, Polycyclic aromatic hydrocarbons in household dust near diesel transport routes, Environ. Geochem. Health 34 (2011) 77–87, https://doi.org/10.1007/s10653-011-9392-4.

[36] L. Wang, J. Deng, L. Yang, T. Yu, Y. Yao, D. Xu, Dynamic analysis of particulate pollution in haze in Harbin city, Northeast China, Open Geosci. 13 (2021) 1656–1667, https://doi.org/10.1515/geo-2020-0327.

[37] W. Li, F. Duan, Q. Zhao, W. Song, Y. Cheng, X. Wang, L. Li, K. He, Investigating the effect of sources and meteorological conditions on wintertime haze formation in Northeast China: a case study in Harbin, Sci. Total Environ. 801 (2021) 149631, https://doi.org/10.1016/j.scitotenv.2021.149631.